FLATNESS BASED TRAJECTORY GENERATION FOR A SYSTEM WITH HEAT-GENERATION TERM SHOWN FOR THE INDUCTIVE HEATING FOR THIXOFORMING

C. Fleck*, A. Schoenbohm*, D. Abel*

* Aachen University of Technology,
Institute of Automatic Control,
Steinbachstraße 54, 52074 Aachen, Germany
Phone: +49 (0)241 8027483, Fax: +49(0)241 8022296
A.Schoenbohm@irt.rwth-aachen.de
Christian_Fleck@yahoo.com

Keywords: Flatness, PDE, Inductive Heating, Heat Transfer, Open-Loop Control

Abstract

An important step in processing of Semi Solid Metals(SSM) is the inductive reheating of the raw material. Using conventional technologies the heating process behaviour is unsatisfactory in terms of reproducibility and disturbance rejection. But reproducibility is a stringent requirement for achieving good quality in the forming process that follows the reheating. In industrial application open loop control is often used but the control trajectories are generated by costly experiments. In order to improve the performance of the open loop control problem and to take constrains on the heating behaviour into consideration, this paper presents a flatness based method to calculate a trajectory for the manipulated variable. The parametrization of the solution is determined by using a Taylor-series expansion around the flat output. In this way a trajectory can be calculated which guarantees that the target temperature is reached as fast as possible and at the same time no overheating of the outer regions occurs. First simulation results are shown for the open loop control case.

1 Introduction

Thixoforming of SSM(Semi Solid Metal) is a new innovative production process that was first proposed by Spencer, Flemings et. al. in the 70^{th}. Materials are formed in the semi solid, semi liquid state. This forming technology allows parts being produced with very good structural material properties as well as complex shape. One disadvantage is the increase in control effort as the material property "semi-solid" exists only in a very small temperature band. The first step in the commonly used thixoforming process is the reheating of a piece of raw material called the billet. The workpiece then is formed on either a forging or a die casting machine. Thixoforming requires the heating of aluminum or other alloy billets to a jelly-like stage between the solidus and liquidus temperature of the material. A uniform billet temperature must be obtained prior to forming in order to obtain good forming results. Although induction heating can meet these requirements and has been used for many years in a variety of metalworking applications, prediction and control of the SSM reheating process is not straightforward. Actually open loop control systems are dominating implementations of the process. This is due to a combination of the complexity of the equations describing the process and the non-linearities associated with the workpiece materials. The induction heating process involves interaction of heat transfer, electrical and magnetic effects. The billet is supposed to be heated to the target temperature as fast as possible and at the same time it must be guaranteed that the outer area of the billet does not overheat and begins to melt prematurely. Conventionally the open loop trajectories are generated by costly experiments in order to achieve the desired state of the billet. In this paper we will show that it is possible to calculate a trajectory for the manipulated variable which satisfies the given constrains on the heating cycle and one can guarantee that the target temperature is reached without overshooting. In figure 1 the principal setup of the induction plant is shown. The plant consists of two interacting subsystems, the induction coil with its magnetic field and the billet with the heat transfer occurring inside. In the following the equations which describe these two subsystems are derived.

2 THE HEATING PROCESS

2.1 The Induction Process

The main part of the plant is the resonant circuit which consists of the capacity connected via a transformer with the induction coil. Energy is fed into the circuit by a converter whose frequency is automatically adapted in order to match the characteristic frequency of the resonant circuit. The heating power is brought into the billet by eddy currents, which are induced mainly near the billet surface by the alternating magnetic field of the induction coil. The manipulated variable of the process is the electrical power of the converter, which in effect means the coil current is varied since the coil voltage is constant.

Figure 2 shows the coil setup with billet. The eddy current density $J_\varphi(r)$ determines the ohmic drop within the billet. If the power distribution of these losses is known it is possible to

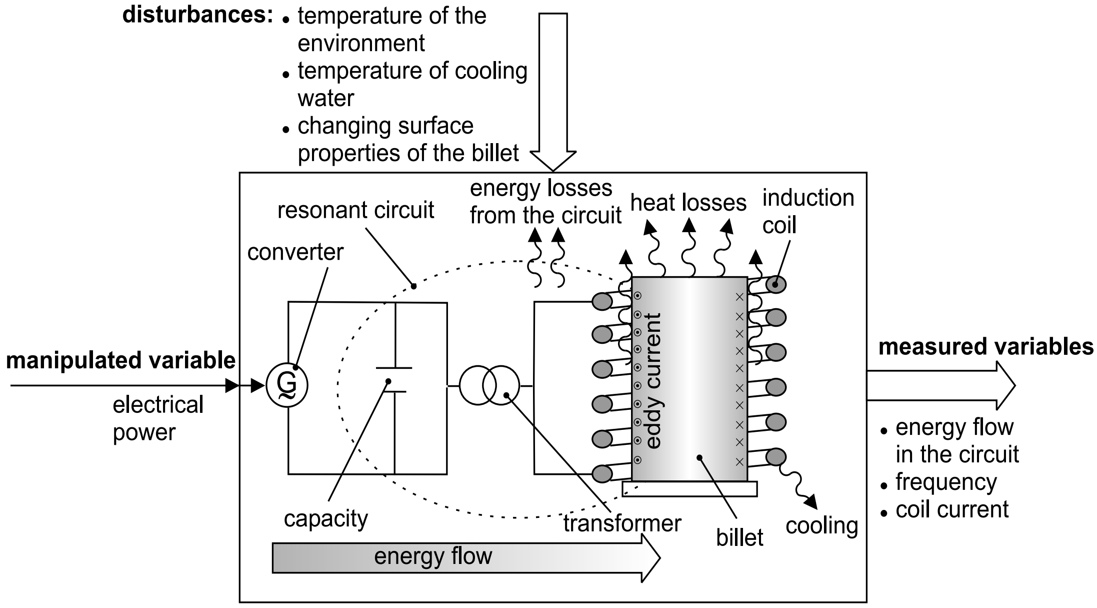

Figure 1: The induction heating plant

calculate the heating of the billet. In order to be able to determine the current density, the magnetic field strength $H_z(r)$

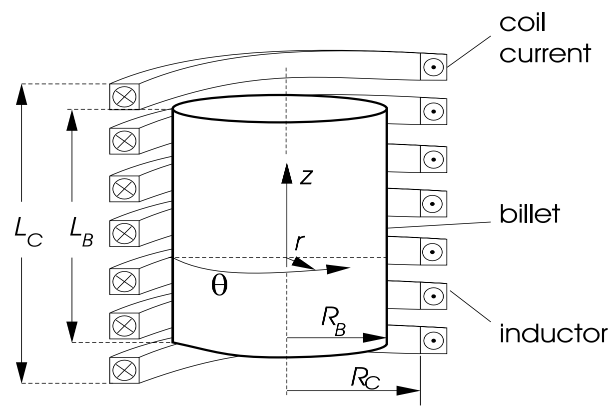

Figure 2: Induction coil with billet

within the billet has to be known. The geometry of the induction coil has been optimized in order to ensure a homogeneous magnetic field distribution inside the coil even at face surfaces [5]. For that reason no variation of the field strength in z direction occurs and since the billet is symmetrical to its middle axis the Maxwell equations in cylindrical coordinates take the following form

$$0 = \frac{\partial^2 H_z}{\partial r^2} + \frac{1}{r}\frac{\partial H_z}{\partial r} - \kappa\mu j\omega H_z \quad (1)$$

$$E_\phi = \frac{1}{\kappa}\frac{\partial H_z}{\partial r} \quad (2)$$

ω is the circular frequency of the coil current, κ the electric conductivity and μ the magnetic permeability. We assume that the variation of the converter power is quite slow compared to the circular frequency ω of the coil current. In that case the quasi-stationary field equations are valid and the variation of the peak value of the coil current can be neglected for the calculation of the field distribution. The solution to 1 is a Bessel function of the first kind and zero order. The eddy current density $J_\varphi(r)$ is related to the magnetic field strength $H_z(r)$ via

$$J_\phi(r) = \kappa E_\phi(r) = -\frac{\partial H_z}{\partial r}. \quad (3)$$

The solution to 3 can be approximated by an exponential function if the penetration depth δ

$$\delta = \sqrt{\frac{2}{\mu\kappa\omega}} \quad (4)$$

is small compared to the radius R_B of the billet. In this case the penetration depth is defined as the distance from the surface at which the current density dropped to 37 percent of its maximum value. Since the heat transfer process is slow compared with the frequency of the induced eddy currents, only the rms-value of the current density $J_\varphi(r)$ can be used for the calculation of the power distribution. The rms-value of the is described by the following equations:

$$J_{rms}(r) = \frac{1}{\sqrt{2}}|J| = J_0 e^{-\frac{(R_B - r)}{\delta}} \quad (5)$$

and

$$J_0 = \frac{H_0}{\delta} \quad \text{and} \quad H_0 = \frac{w}{L_C} I_0 \quad (6)$$

w describes the number of coil windings, L_C the length of the coil and I_0 the peak value of the coil current. The induced volume power density $\dot{\Phi}(r)$ is described by the following term

$$\dot{\Phi}(r) = \frac{1}{\kappa} J_{rms}^2 = \Phi_0 e^{-2\frac{(R_B - r)}{\delta}} = g(t) \cdot f(r)$$

$$\text{with } \mathrm{f(r)} = \mathrm{e}^{-2\frac{(\mathrm{R_B - r})}{\delta}},\ \mathrm{g(t)} = \frac{\mathrm{w}^2}{\kappa\delta^2 \mathrm{L_C}} \mathrm{I_0^2(t)} \quad (7)$$

In figure 3 the behaviour of the current and volume power density in dependency of the radius r are shown.

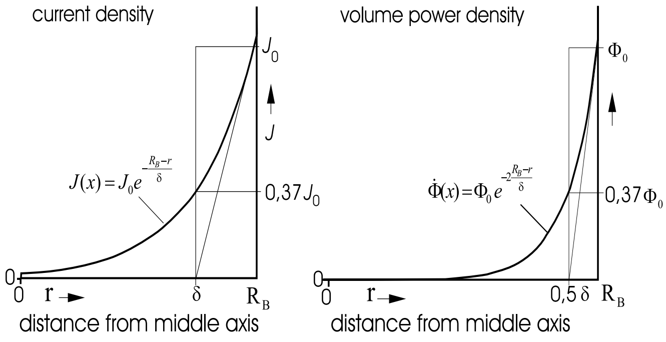

Figure 3: Eddy Current and volume power density

2.2 The Heat Transfer Equations

To be able to calculate the trajectory for the converter power, the thermal behaviour of the billet has to be described. Considering the cylindrical symmetry of the billet (see figure 2), the heat transfer inside the billet represents a two dimensional problem that can be described by the following equation in cylindrical coordinates:

$$\rho c_v \frac{\partial \vartheta}{\partial t} = \frac{1}{r}\frac{\partial}{\partial r}\left(r\lambda\frac{\partial \vartheta}{\partial r}\right) + \frac{\partial}{\partial z}\left(\lambda\frac{\partial \vartheta}{\partial z}\right) + \dot{\Phi}(r) \quad (8)$$

where $\dot{\Phi}(r)$ is the heat-generation term which represents the induced volume power density described by 7. ρ describes the density, c_v represents the specific heat capacity and λ corresponds to the heat conduction coefficient of the material. These parameters are regarded to be constant and thus any temperature dependencies are neglected. Since the coil geometry ensures a homogeneous magnetic field strength along the z axis and heat losses occur mainly along the jacket of the billet, the heat transfer in axial direction can be neglected and 8 can be written as follows:

$$\begin{aligned}\rho c_v \frac{\partial \vartheta(r,t)}{\partial t} &= \lambda\frac{1}{r}\frac{\partial}{\partial r}\left(r\frac{\partial \vartheta(r,t)}{\partial r}\right) + \dot{\Phi}(r) \quad (9)\\ &= \lambda\frac{1}{r}\frac{\partial \vartheta(r,t)}{\partial r} + \lambda\frac{\partial^2 \vartheta(r,t)}{\partial r^2} + g(t)\cdot f(r)\end{aligned}$$

At the beginning of the heating cycle the billet temperature is supposed to be uniformly equal to the environment temperature ϑ_e, which leads to the initial condition:

$$\vartheta(r,0) = \vartheta_e \quad ,0 \le r \le R_B. \quad (10)$$

Due to the rotational symmetry with respect to the point $r = 0$, no heat transfer through the axis can occur which leads to the first boundary condition:

$$\left.\frac{\partial \vartheta(0,t)}{\partial r}\right|_{r=0} = 0 \quad ,t \ge 0. \quad (11)$$

The second boundary condition is determined by the heat flow from the jacket to the environment, i.e. for $r = R_B$, and is described by

$$\dot{Q}_s(t) = \frac{\partial \vartheta(R_B,t)}{\partial r} = -\frac{\alpha}{\lambda}\left(\vartheta(R_B,t) - \vartheta_e(t)\right) \quad ,t \ge 0 \quad (12)$$

where α denotes the heat-transfer coefficient. $\vartheta(R_B,t) = \vartheta_s(t)$ corresponds to the temperature of the billet jacket and ϑ_e to the environment temperature which is supposed to be constant. Due to the oxidation of the billet surface radiation losses can be neglected. Without loss of generality we set $\vartheta_e = 0$ in following.

3 DETERMINATION OF FLAT OUTPUTS

The approach used in this paper is based upon the concept of flatness of systems which has been introduced by [3]. Using the flat outputs it is possible to calculate trajectories for the system which guarantees that the outputs follow the desired behaviour. There are a lot of applications of flatness to systems with concentrated parameters [4] and lately to distributed systems too. Examples of flatness for heat transfer problems can be found at [2] and [1]. These systems are boundary controlled, i.e. the system is influenced by a final controlling element at the boundary of the system.
The system described by 9 is controlled by the heat-generation term $\dot{\Phi}(r)$ and thus the results mentioned before cannot be applied directly to the given problem. The flat output of the system can be determined if we identify a place where by using the boundary conditions and the behaviour of the temperature in that place all derivatives of the pde are determined.
If we regard the point $r = 0$ of the system we can determine all derivation terms of the pde by using the first boundary condition 11 and fixing the behaviour for $g(t)$ and $\theta(0,t)$ over time. Thus these variables are candidates for the components of the flat output. But the system is only flat if the dimension of the flat output is equal to the dimension of the manipulated variables. Obviously $g(t)$ is the first manipulated variable and the environment temperature $\vartheta_e(t)$ can be interpreted as the second one since it affects the system behaviour as well. $\vartheta_e(t)$ cannot be influenced but is supposed to be known. That means the system is flat and the solution to 9 can be parametrized by the temperature at the axis $y_{f1}(t) = \vartheta(0,t)$ and the coil current $yf2(t) = g(t)$.
In order to determine the parametrization, we develop the solution $\vartheta(r,t)$ to 9 in a Taylor-series around the point $r = 0$:

$$\begin{aligned}\vartheta(r,t) = \vartheta(0,t) &+ \left.\frac{\partial \vartheta(r,t)}{\partial r}\right|_{r=0}\frac{r}{1!} + \left.\frac{\partial^2 \vartheta(r,t)}{\partial r^2}\right|_{r=0}\frac{r^2}{2!}\\ &+ \left.\frac{\partial^3 \vartheta(r,t)}{\partial r^3}\right|_{r=0}\frac{r^3}{3!} + \left.\frac{\partial^4 \vartheta(r,t)}{\partial r^4}\right|_{r=0}\frac{r^4}{4!} + \cdots\end{aligned} \quad (13)$$

Due to the symmetry of the given problem, the solution $\vartheta(r,t)$ to 9 must be an even function with respect to the point $r=0$. This means that all odd derivatives with respect to r at the point $r=0$ must be equal to zero:

$$\left.\frac{\partial^{2n+1}\vartheta(r,t)}{\partial r^{2n+1}}\right|_{r=0} = 0 \quad ,\text{for } n = 0..\infty \tag{14}$$

Now only even derivation terms occur in 13 and have to be calculated in order to determine the solution. By rearranging 9 one obtains an expression for the second derivation with respect to r:

$$\frac{\partial^2\vartheta(r,t)}{\partial r^2} = \frac{\rho c_v}{\lambda}\frac{\partial\vartheta(r,t)}{\partial t} - \frac{1}{r}\frac{\partial\vartheta(r,t)}{\partial r} - \frac{1}{\lambda}f(r)\cdot g(t). \tag{15}$$

In order to be able to substitute the corresponding expression in the Taylor series 13, equation 15 must be evaluated at the point $r=0$:

$$\begin{aligned}
\lim_{r\to 0}\left(\frac{\partial^2\vartheta(r,t)}{\partial r^2}\right) &= \frac{\rho c_v}{\lambda}\left.\frac{\partial\vartheta(r,t)}{\partial t}\right|_{r=0} - \lim_{r\to 0}\left(\frac{1}{r}\frac{\partial\vartheta}{\partial r}\right) \\
&\quad -\frac{1}{\lambda}f(0)\cdot g(t) \\
\left.\frac{\partial^2\vartheta(r,t)}{\partial r^2}\right|_{r=0} &= \frac{\rho c_v}{\lambda}\left.\frac{\partial\vartheta(r,t)}{\partial t}\right|_{r=0} - \left.\frac{\partial^2\vartheta(r,t)}{\partial r^2}\right|_{r=0} \\
&\quad -\frac{1}{\lambda}f(0)\cdot g(t) \\
&= \frac{1}{2}\left(\frac{\rho c_v}{\lambda}\frac{\partial\vartheta(0,t)}{\partial t} - \frac{1}{\lambda}f(0)\cdot g(t)\right)
\end{aligned} \tag{16}$$

The higher order derivatives in 13 can be determined by the $2n^{th}$ derivation of 15 and then evaluating the expression at $r=0$.

$$\begin{aligned}
\frac{\partial^{2n+2}\vartheta(r,t)}{\partial r^{2n+2}} &= \frac{\rho c_v}{\lambda}\underbrace{\frac{\partial^{2n}}{\partial r^{2n}}\left(\frac{\partial\vartheta}{\partial t}\right)}_{A} - \underbrace{\frac{\partial^{2n}}{\partial r^{2n}}\left(\frac{1}{r}\frac{\partial\vartheta}{\partial r}\right)}_{B} \\
&\quad -\frac{1}{\lambda}\underbrace{\frac{\partial^{2n}}{\partial r^{2n}}\left(f(r)\cdot g(t)\right)}_{C} \\
&\quad \text{with } n = 0..\infty
\end{aligned} \tag{17}$$

Evaluating this expression at $r=0$ yields:

$$\begin{aligned}
\lim_{r\to 0} A &= \frac{\partial}{\partial t}\left(\frac{\partial^{2n}\vartheta(0,t)}{\partial r^{2n}}\right) \\
\lim_{r\to 0} B &= \frac{1}{(2n+1)}\frac{\partial^{2n+2}\vartheta(0,t)}{\partial r^{2n+2}} \\
\lim_{r\to 0} C &= g(t)\frac{\partial^{2n}f(0)}{\partial r^{2n}} \\
\frac{\partial^{2n+2}\vartheta(0,t)}{\partial r^{2n+2}} &= \frac{2n+1}{2n+2}\left(\frac{\rho c_v}{\lambda}\frac{\partial}{\partial t}\left(\frac{\partial^{2n}\vartheta(0,t)}{\partial r^{2n}}\right)\right. \\
&\quad \left. -\frac{1}{\lambda}g(t)\frac{\partial r^{2n}f(0)}{\partial r^{2n}}\right)
\end{aligned} \tag{18}$$

By using the following substitution, a recursive formula for the calculation of the derivatives can be determined:

$$\begin{aligned}
a_{2n}(t) &= \frac{\partial^{2n}\vartheta(0,t)}{\partial r^{2n}} \\
a_{2n+2}(t) &= \frac{2n+1}{2n+2}\left(\frac{\rho c_v}{\lambda}\frac{\partial a_{2n}(t)}{\partial t} - \frac{1}{\lambda}g(t)\frac{\partial^{2n}f(0)}{\partial r^{2n}}\right)
\end{aligned} \tag{19}$$

For $n=0$, $a_0(t)=\vartheta(0,t)$ is determined and the recursion formula can be used to calculate the higher order derivatives of 15. Thus the Taylor series 13 can be written as follows:

$$\begin{aligned}
\vartheta(r,t) &= a_0(t) + \frac{a_2(t)}{2!}r^2 + \frac{a_4(t)}{4!}r^4 + \cdots \\
&= \sum_{\mathrm{n}=0}^{\infty}\frac{\mathrm{a_{2n}}(t)}{(2n)!}r^{2n}
\end{aligned} \tag{20}$$

with

$$\begin{aligned}
a_0(t) &= \vartheta(0,t) \\
a_2(t) &= \frac{1}{2}\left(\dot{a}_0(t) - g(t)\,f(0)\right) = \frac{1}{2}\left(\dot{\vartheta}(0,t) - g(t)\,f(0)\right) \\
a_4(t) &= \frac{3}{4}\left(\dot{a}_2(t) - g(t)\frac{\partial^2 f(0)}{\partial r^2}\right) \\
&= \frac{3}{4}\left(\frac{\partial}{\partial t}\left(\frac{1}{2}\left(\dot{\vartheta}(0,t) - g(t)\,f(0)\right)\right) - g(t)\frac{\partial^2 f(0)}{\partial r^2}\right) \\
&= \frac{3}{4}\left(\frac{1}{2}\ddot{\vartheta}(0,t) - \frac{1}{2}\dot{g}(t)\,f(0) - g(t)\frac{\partial^2 f(0)}{\partial r^2}\right) \\
&\vdots
\end{aligned} \tag{21}$$

These calculations show that the solution $\vartheta(r,t)$ is parametrized if all the $a_{2n}(t)$ are known. As 21 shows, the $a_{2n}(t)$ are dependent on $\vartheta(0,t)$ and its time derivatives, $g(t)$ and its time derivatives and $f(r)$ and its derivatives with respect to r. Since $f(r)$ is known from 7, the Taylor series 20 is determined if $\vartheta(0,t)$ and $g(t)$ are known. This means that the solution $\vartheta(r,t)$ is parametrized by the middle temperature of the billet $y_{f1}(t)=\vartheta(0,t)$ and the coil current $yf2(t)=g(t)$ as mentioned before.

The aim of the control is to ensure that the flat output $y_{f1}(t)$ follows a desired trajectory by determining the needed trajectory of the input variable $g(t)$. The environment temperature $\vartheta_e(t)$ cannot be manipulated and is supposed to be constant. Only a trajectory for the temperature at the middle axis $\vartheta(0,t)$ can be fixed since the second flat output $g(t)$ is at the same time the manipulated variable.

Usually the control trajectory can be calculated without integration, but since the system is not boundary controlled, integration is needed in order to determine the trajectory $g(t)$. By inserting the Taylor series 20 into the second boundary condition 12, it is possible to calculate $g(t)$ in such manner that a given trajectory for $y_{f1}(t) = \vartheta(0,t)$ is fixed:

$$\begin{aligned} \frac{\partial\vartheta(R_B,t)}{\partial r} &= -\frac{\alpha}{\lambda}\vartheta(R_B,t) \\ \sum_{\mathrm{n}=1}^{\frac{N}{2}} \frac{\mathrm{a_{2n}}(t)}{(2n-1)!}R_B^{2n-1} &= -\sum_{\mathrm{n}=0}^{\frac{N}{2}} \frac{\mathrm{a_{2n}}(t)}{(2n)!}R_B^{2n} \end{aligned} \quad (22)$$

If the Taylor series is truncated at an order of N, we obtain a linear ODE of $(\frac{N}{2}-1)^{\text{th}}$ order with $g(t)$ as the dependent variable. The solution to this ODE provides the desired trajectory for $g(t)$ which then guarantees that the flat output $y_{f1}(t)$ follows the predetermined trajectory. The ODE for $g(t)$ can be limited to the first couple of derivations since the high order derivations are weighted by the factor $\frac{1}{n!}$ of the Taylor-series and thus have little effect for the solution.

4 NUMERICAL SIMULATIONS

In this section the results of the presented method are shown on the basis of numerical simulations concluded with Maple. The Taylor series is being developed up to an order of 8. For sake of simplicity all material constants are set to one.
For the flat output $y_{f1}(t)) = \vartheta(0,t)$ the following trajectory is desired. The given trajectory is a polynomial of sufficient smoothness in order to avoid a non smooth control trajectory:

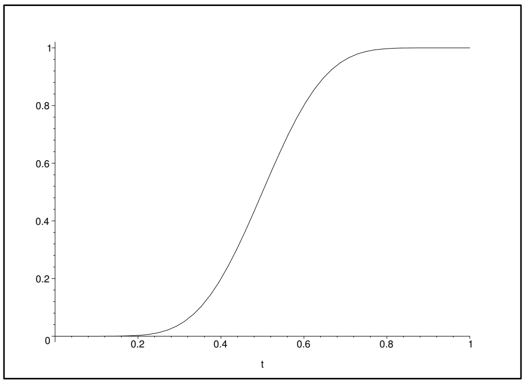

Figure 4: Desired trajectory for $y_{f1}(t)$

The following figure shows the calculated trajectory for the manipulated variable $g(t)$:

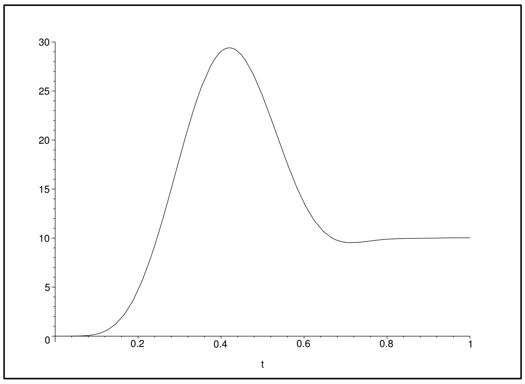

Figure 5: Calculated trajectory for $g(t)$

Below he numerical solution and the Taylor series of an order of 8 for the calculated $g(t)$ are shown :

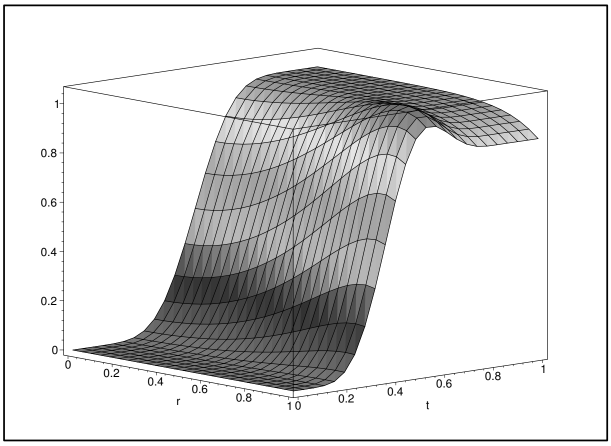

Figure 6: Numerical solution for $\vartheta(r,t)$

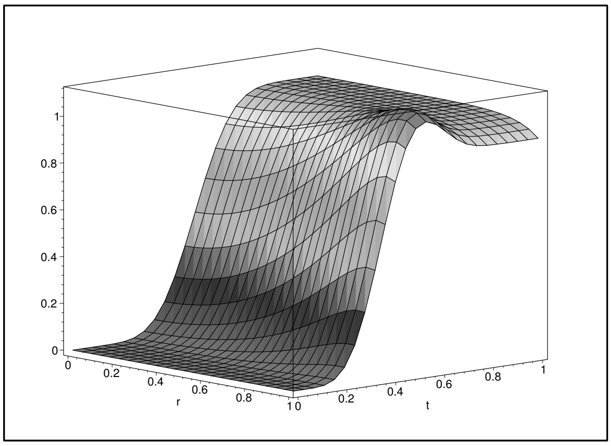

Figure 7: Taylor series for $\vartheta(r,t)$

It can be seen that the numerical solution and the Taylor series match each other quite well. There is still a small deviation of the numerical solution from the Taylor solution towards $r =$

1 and the calculated course for $g(t)$ leads to a slightly higher steady state temperature as the Taylor series. But this effect can be reduced by using a higher order Taylor series.
The curve below shows the desired temperature behaviour for a transition time of 10 seconds:

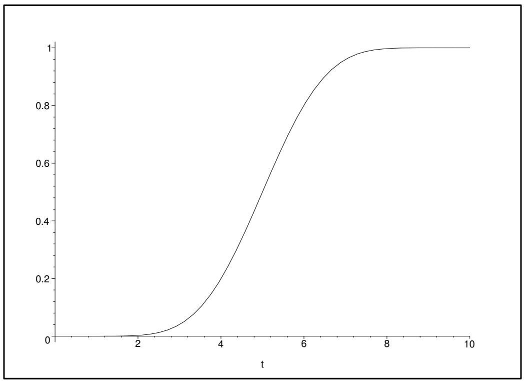

Figure 8: Desired trajectory for $y_{f1}(t)$

The following figure shows the calculated trajectory for the manipulated variable $g(t)$:

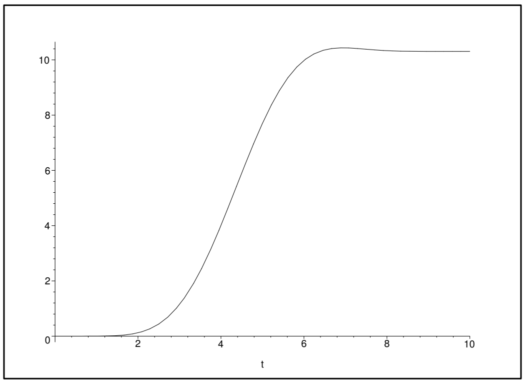

Figure 9: Calculated trajectory for $g(t)$

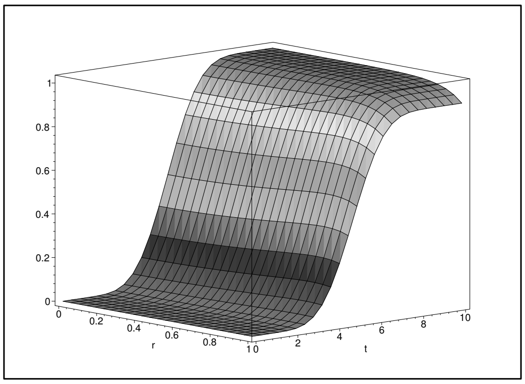

Figure 10: Numerical solution for $\vartheta(r,t)$

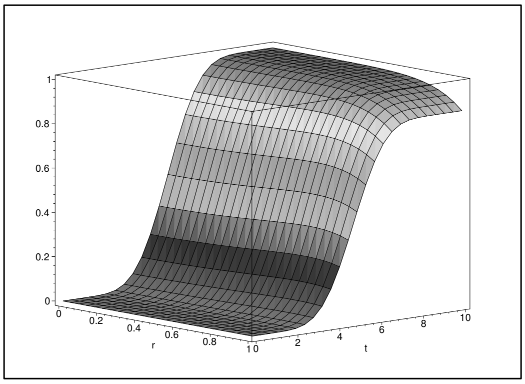

Figure 11: Taylor series for $\vartheta(r,t)$

5 CONCLUSION

We presented a method to determine the flat outputs for a distributed system which is manipulated by a heat-generating term. The parametrization of the solution by means of the flat output has been shown and the calculated control trajectory has been applied to the system via numerical simulations. These simulations indicate that it is possible to achieve the desired behaviour of the middle temperature by applying the calculated trajectory to the system.

6 ACKNOWLEDGEMENTS

The authors gratefully acknowledge the financial support of the Deutsche Forschungsgemeinschaft (DFG) within the Collaborative Research Center (SFB) 289 ”Forming of metals in the semi-solid state and their properties”.

References

[1] J.Rudoph A.F.Lynch. Flachheitsbasierte Randsteuerung parabolischer Systeme mit verteilten Parametern. *at-Automatisierungstechnik*, 48:478–486, 2000.

[2] P. Rouchon B. Laroche, P. Martin. Motion planning for the heat equation. *Int. J. Robust Nonlinear Control*, 10:629–643, 2000.

[3] Ph. Martin P. Rouchon M. Fliess, J. Levine. Flatness and defect of nonlinear systems: Introductory theory and examples. *Int. J. of Control*, 61:1327–1361, 1995.

[4] Ph. Martin, R.M. Murray and P. Rouchon. *Flat Systems*, pages 211–264. Bastin,G and Gevers, M, 1997.

[5] R. Sebus. *Entwicklung eines Verfahrens zur induktiven Erwärmung von Aluminiumlegierung in den thixotropen Zustand*. Shaker Verlag, 2001.